

EXPERIMENTAL AND THEORETICAL ANALYSIS OF SCANNING LASER EPITAXY APPLIED TO NICKEL-BASED SUPERALLOYS

R. Bansal, R. Acharya, J. J. Gambone, and S. Das

Woodruff School of Mechanical Engineering, Georgia Institute of Technology
Atlanta, GA 30332-0405

Abstract

This paper reports on the experimental development and the theoretical analysis of the scanning laser epitaxy (SLE) process that is currently being investigated and developed at the Georgia Institute of Technology. SLE is a laser-based manufacturing process for deposition of equiaxed, directionally solidified and single-crystal nickel superalloys onto superalloy substrates through the selective melting and re-solidification of superalloy powders. The thermal modeling of the system, done in a commercial CFD software package, simulates a heat source moving over a powder bed and considers the approximate change in the property values for consolidating CMSX-4 nickel superalloy powder. The theoretical melt depth is obtained from the melting temperature criteria and the resulting plots are presented alongside matching experimental micrographs obtained through cross-sectional metallography. The influence of the processing parameters on the microstructural evolution, as evidenced through observations made from the micrographs, is discussed. This work is sponsored by the Office of Naval Research, through grants N00173-07-1-G031 and N00014-10-1-0526.

Introduction

In order to increase the operating temperature of gas turbine aero engines, investment cast equiaxed turbine component parts are now often replaced with directionally solidified components that have either columnar or single crystal (SX) morphology. During the operation of these SX turbine blades, damage and wear at their leading tip occurs which limits the lifetime of the SX components and necessitates the replacement of the numerous airfoils within the engines. Due to the high cost of producing SX cast turbine blades, the cost of replacing each blade is several thousand dollars. With each engine containing several hundred blades, the cost to replace every one can reach hundreds of thousands of dollars. Hence, it is of great interest to develop a process which will restore the single crystal microstructure at the damaged location and allow for the blades to be reused rather than scrapped and replaced.

Such repairs were first attempted using processes such as Tungsten Inert Gas Welding and Laser melting using a defocused laser (United Technologies Corporation). However, these processes either could not create single crystal deposits, could not be applied to complex geometries, or suffered from crack formation[1]. Laser Engineered Net Shaping, Laser Cladding and Epitaxial Laser Metal Forming have more recently attempted to restore single crystal airfoils to working condition[2]. However, crack formation, columnar to equiaxial transition (CET), oriented to misoriented transition (OMT) and stray grain formation hinders the applicability of all of the above processes to this particular tip repair process [1, 3-5]. This work focuses on the

further development of a new process, scanning laser epitaxy (SLE), by which arbitrary SX high value components can be repaired.

SLE is a laser-based manufacturing process for deposition of equiaxed, directionally solidified and single-crystal nickel superalloys onto superalloy substrates through the selective melting and re-solidification of superalloy powders. In this particular implementation of the process, a laser beam guided by a set of high-speed galvanometer scanners allows for tight control of the amount of energy being applied to the top of the powder bed as well as the speed at which the melt pool moves across the substrate. Under the proper operating conditions and with enough substrate re-melt, the solidification of the powder melt pool will follow the morphology of the underlying substrate, allowing for directional and even SX growth.

Current work focuses on experimentation used to establish an optimal operating range for the various process parameters in the SLE blade repair process. The effects of these different processing parameters on build quality are also examined from the microstructural point of view. In particular, the change of grain structure and morphology along with any angular misorientation is studied in detail. A thermal model has also been incorporated in the analysis to predict the melt depth considering the approximate property changes in the powder bed during melting. The model simulates the entire laser scan path and gives some fundamental idea about the effect of repeat scans on preheating, the approximate melt depth and the temperature distribution in the powder bed and substrate.

Experimental

Due to its frequent use in modern SX airfoil designs, the nickel-based superalloy CMSX-4 was chosen as the material to be used in this evaluation of the SLE process. The CMSX-4 powder, listed in Table 1, was produced by Praxair Surface Technologies using an atomization process and had a particle size ranging from 85-150 μ m. Initially, the process was tested on rectangular SX cast CMSX-4 coupons having dimensions of 35.56mm x 10.16mm x 2.54mm. Each substrate was placed into a 35.56mm x 10.16mm recession cut into an Inconel 625 base plate.

Table 1. Chemical Compositions (wt%) of CMSX-4

	Cr	Co	Mo	Re	W	Al	Ti	Ta	Hf	Ni
CMSX-4	7.6	9.3	0.4	1.0	2.0	12.6	1.3	2.2	0.03	Bal

During preliminary testing the powder was deposited in various thicknesses, between 1 and 2mm, to find the ideal height of deposit. The powder was held in place above the substrate using wells cut into a Cotronics foam ceramic board that is resistant to thermal shock.

After the samples were prepared, they were placed into a Terra Universal atmospheric glove box which was then purged with argon. A 1064nm 2kW Nd:YAG laser beam was used in conjunction with a Cambridge Technologies galvanometer scanner to focus the beam to a diameter of 1.5mm at the top of the substrate. A consistent raster scan pattern across the width of the sample was used to propagate a linear melt pool across each substrate. Three variables were altered between each experimental run: laser power, scan speed, and the number of repeated

scans at the start of the raster pattern. Table 2 lists the operating ranges for each of the parameters.

Table 2. Process parameter ranges found to produce well formed CMSX-4 deposits.

Process Parameter	Range
Powder Thickness	1 – 2 mm
Laser Power	400 – 600 W
Scan Speed	150 – 250 mm/sec
Initial Repeat Scans	50 – 150

The laser power and speed of the scan were both used to control the amount of energy being applied to the sample during the raster scan pattern. The number of initial repeat scans affected the formation of a melt pool at the start of the substrate as well as preheat temperature of the entire substrate. Sufficient preheat was required in order to form a proper fusion bond across the whole substrate. Without sufficient preheating, the melt pool would not wet the surface of the underlying substrate and voids were formed along the interface.

Microstructural Investigation

Each sample was sectioned along the length and width to allow for views of the microstructure. Using a Buehler automated saw, each sample was first cut lengthwise, and then sectioned by multiple widthwise cuts, as shown in Figure 1.

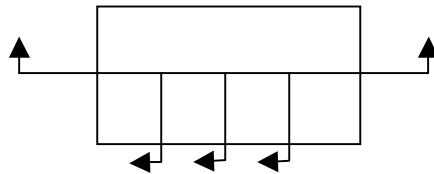


Figure 1. Sections used in metallographic analysis

Each section was mounted in Bakelite and ground to a smooth finish; starting at 80 grit paper and progressively increasing the grit to 1200. The samples then underwent a rough polishing operation with 5 μ m and 3 μ m diamond solutions. Finally, the samples are smoothed to a mirror finish using a 0.5 μ m silica suspension. The polished samples were then exposed to Kalling's No. 2 etchant composed of 50ml Ethanol, 50ml HCl and 2.5g CuCl₂ in order to expose the microstructure for microscopy. Imaging was then completed using a Leica DM6000 Optical Microscope at 100x magnification.

As demonstrated by the sample in Figure 2, many sections showed a full metallographic bond along the entire length of the sample. The transition from the cast CMSX substrate to the laser processed material is indicated by the sharp change in dendrite size. Also of note are the fully dense porosity free deposit, and the lack of any hot tearing or stress cracking. These traits are consistently found in samples manufactured using the SLE process and are necessary for their implementation on any commercial engine.

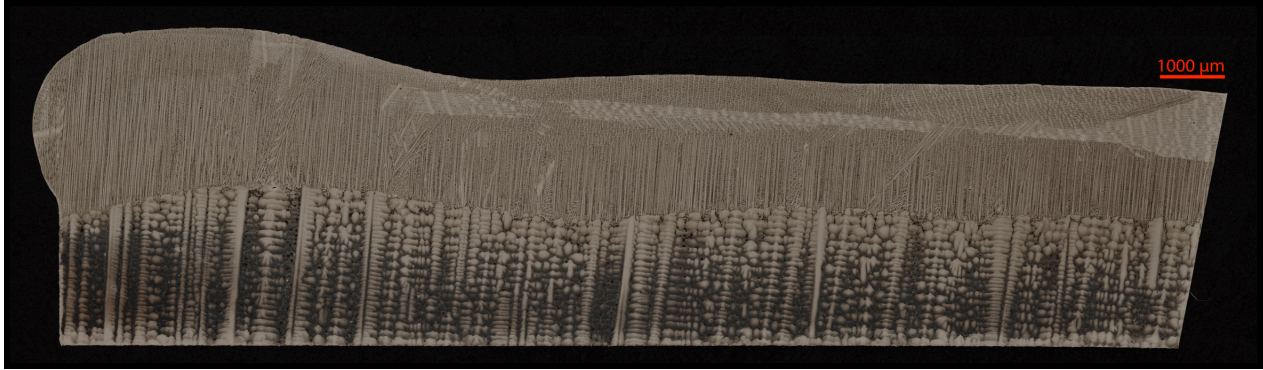


Figure 2. Representative lengthwise section of the first half of a CMSX-4 sample with the starting edge on the left side of the image

Figure 3 provides a detailed view of the transition from the coarse dendrites of the cast CMSX substrate to the finer dendrite size created during the experiments. The dendrite arm spacing of the added material is found to be ~15 times finer than in the substrate due to a focused heat input and the increased speed at which the SLE process occurs resulting in a very high temperature gradient as compared to the casting process. The orientation of the columnar growth in the newly deposited material also shows little to no angular misorientation as compared to the underlying substrate.

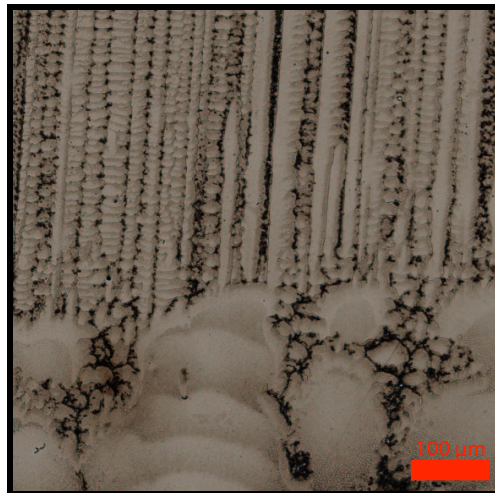


Figure 3. Coarse to fine grain transition marking the transition from substrate to deposit

Figure 4 provides a closer look at the transition from single crystal growth with [001] directionality to a shift in orientation. This change is known as oriented to misoriented transition (OMT) and is caused by a change in direction of the temperature gradient as the substrate becomes increasingly hot toward the end of the scan.

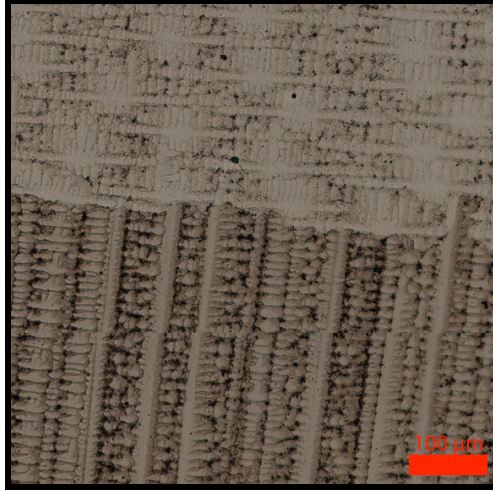


Figure 4. Oriented to misoriented transition

On some samples, the top of the deposit suffered from an area of equiaxial grain growth. This columnar to equiaxial transition (CET) is due to the increase in isotherm velocity near the surface and a decrease in the temperature gradient which causes formation of a constitutionally undercooled zone [1]. Despite these regions of misoriented and equiaxial grain growth, most samples showed an SX deposit height of at least 500µm. In production parts, the misoriented and equiaxial dendrite formations would be removed via a grinding operation or via a re-melt operation if multiple layers were to be built.

Modeling

Computer simulations were conducted to enable further understanding of the heating and cooling process that leads to the microstructure found in the samples. Initial efforts focused on a thermal model to predict the melt depth along the length of the sample.

A multi-domain model with temperature-dependent property values was used to simulate the thermal aspect of the model and to predict the melt depth. The mesh for the given problem was generated in the ANSYS Mesher. The element count for the given case was around 110k with all hexagonal elements and skew not exceeding 0.44. The problem was solved in the finite volume based CFD solver, ANSYS CFX, without incorporating the fluid convection.

The equation solved for the given model is shown in Equation 1,

$$\rho \frac{\partial(\rho H)}{\partial t} = \nabla \cdot (K \nabla T) + S_0 \quad \text{Eq. 1}$$

where, ρ = Density, H = Enthalpy, K = Thermal conductivity, S_0 = Heat source. A convection boundary condition was applied along the entire external surface to model the convection heat loss with a high convection coefficient at the top surface (100 W/m²K).

The powder bed properties were dynamically modified with the local temperature value as listed in Table 3.

Table 3. Powder bed properties for CMSX-4

T (K)	ρ (kg/m ³)	K (W/mK)	C _p (J/kgK)
300	4350.59	14.2387	929.94
1636	8700	28.4512	815.88

The moving heat source was modeled with the total input laser power being confined within a 1.5mm beam diameter Gaussian distribution. The laser initially scans the starting edge for a specified number of iterations, listed as the number of repeat scans, before starting the raster scan over the remainder of the substrate. The moving heat source was simulated following the same path in CFX. The heat source value was also varied to approximate the change in absorptivity for CMSX-4 powder in the final sintered stage [6].

The problem was modeled in CFX using the multi-domain approach, with conservation of H-energy being maintained at the interface of the substrate and powder bed. The model did not consider the latent heat since phase change was not yet incorporated.

The temperature distribution after the initial repeat scans for one particular case is shown in Figure 5. The bulk preheating obtained, as calculated from the volume averaged quantity, is 47 K for the given case.

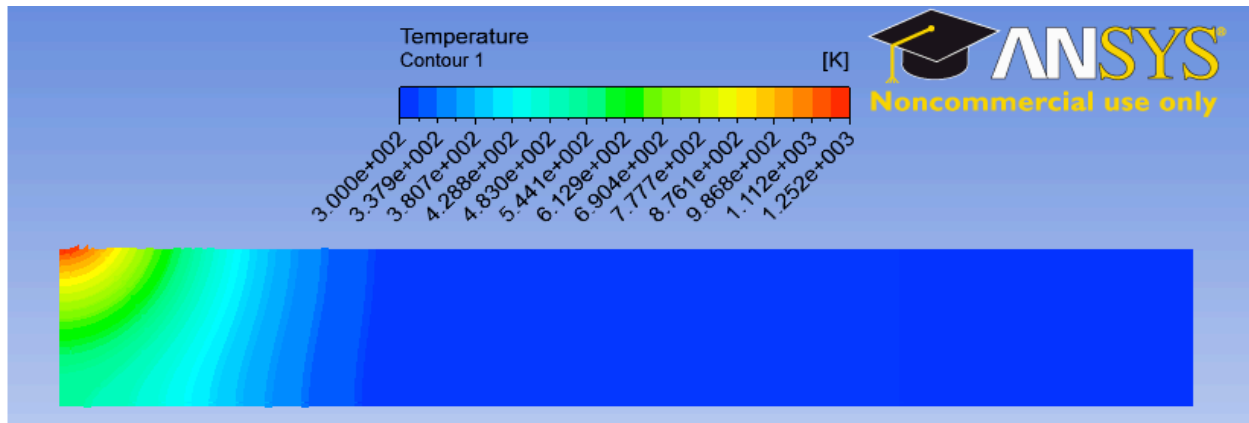


Figure 5. Simulated temperature distribution after completing the repeat starting edge scans

The melt depth was computed via tracking of the maximum temperature value obtained at any given plane and comparing it with the liquidus temperature for CMSX-4. The simulated melt depth was then compared with the experimentally obtained melt depth and a reasonable match was obtained over most of the scan length, as shown in Figure 6.

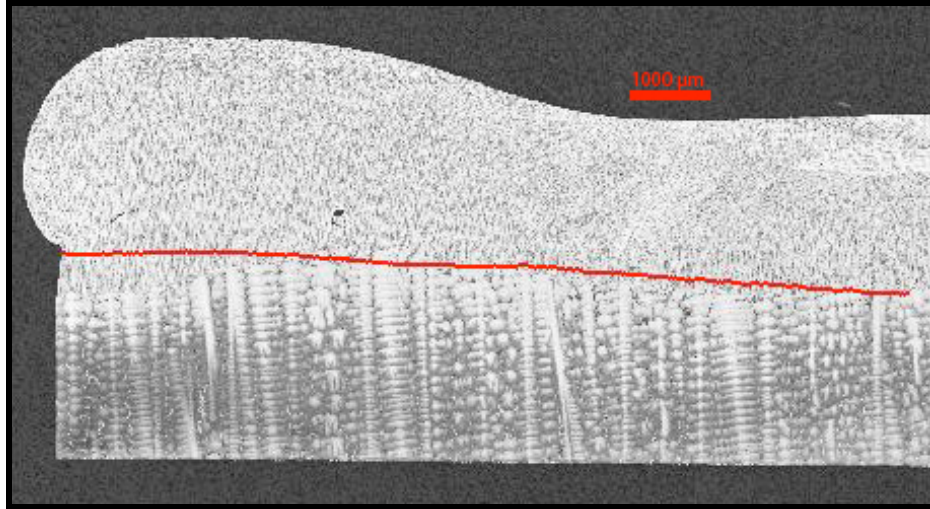


Figure 6. Plot of the simulated melt depth, indicated by the red line, superimposed on top of an experimental micrograph run at identical processing parameters

Inaccuracy in the model may arise due to not incorporating the phase change, the radiation loss from the boundary and approximate convection coefficient used in the model. Misalignment of the scan path adopted in the model as compared to the actual experimental scan path may also play a role in the relatively larger inaccuracy in the predicted melt depth at the starting edge of the sample. Future simulation work will involve modeling of the microstructure formed from the melt fraction and temperature gradient data.

Conclusions

The intention of the current work was to establish an operating range of input parameters which will create a favorable temperature gradient and solidification velocity that promotes SX morphology. This was complemented by developing a thermal model which could successfully predict the melt depth and to estimate the level of preheating obtained due to starting edge repeat scans.

The current effort also leads to some important microstructural observations. The resultant microstructure was substantially finer compared to the investment cast substrate. The deposits did not show cracking or hot tearing once the proper operating range of process parameters was established. The low-angle misorientation did not exceed the allowable range, as evidenced by the microstructural analysis. The height of columnar grain growth obtained was restricted by a flip in grain growth direction near the top trailing edge of the deposit (OMT) as well as due to the formation of an equiaxed cap (CET). Due to the large height of the SX portion of the deposits produced via SLE, the misoriented and equiaxed portions at the top of the deposit can be removed using a post processing operation while still leaving a significant amount of newly deposited SX material.

Future work will encompass the reduction of these misoriented and equiaxed regions near the top of the deposits by utilizing feedback control in order to better control the temperature gradients present during processing. The feedback control will be based upon the

modeling of microstructural formation from the simulated melt fraction and temperature gradient data.

Acknowledgements

The authors of this paper would like to thank the Office of Naval Research, and in particular Program Managers Dr. Khershed Cooper and Dr. Ralph Wachter, for their support under grants N00173-07-1-G031, N00014-10-1-0526, N00014-10-1-0756, and N00014-11-1-0670.

References

1. Gaumann, M., *Epitaxial Laser Metal Forming of a Single Crystal Superalloy*, 1999.
2. MORTENSEN, et al., *Functionally graded metals and metal-ceramic composites: Part 1 processing*. Vol. 40. 1995, London, ROYAUME-UNI: Maney.
3. Anderson, T.D., J.N. DuPont, and T. DebRoy, *Origin of stray grain formation in single-crystal superalloy weld pools from heat transfer and fluid flow modeling*. Acta Materialia, 2010. **58**(4): p. 1441-1454.
4. Mokadem, S., *Epitaxial Laser Treatment of Single Crystal Nickel Base Superalloys*, 2004.
5. Mokadem, S., et al., *Laser Repair of Superalloy Single Crystals with Varying Substrate Orientations*. Metallurgical and Materials Transactions A, 2007. **38**(7): p. 1500-1510.
6. Hauser, C. and T.H.C. Childs, *Raster scan selective laser melting of the surface layer of a tool steel powder bed*. Proceedings of the Institution of Mechanical Engineers, Part B: Journal of Engineering Manufacture, 2005. **219**(4): p. 379-384.